



Generation of KS-487 as a novel LRP1-binding cyclic peptide with higher affinity, higher stability and BBB permeability

Kotaro Sakamoto

Research & Development Department, Ichimaru Pharcos Company Limited, 318-1 Asagi, Motosu, 501-0475, Gifu, Japan

ARTICLE INFO

Keywords:

LRP1
RMT
BBB
CNS
DDS
Cyclic peptide

ABSTRACT

The blood–brain barrier (BBB) is a major hurdle in drug discovery for central nervous system (CNS) disorders. Particularly, mid-size molecules and macromolecules (e.g., peptides and antibodies) that modulate intractable drug targets such as protein–protein interaction are prevented from entering the CNS via BBB. The receptor-mediated transcytosis (RMT) pathway has been examined to deliver these molecules to CNS. Among the receptors, low-density lipoprotein receptor-related protein 1 (LRP1) has been emerged as one of the promising receptors for RMT. Although several LRP1-binding peptides have been reported, no drugs are available on the market based on the combination of reported LRP1-binding peptides and therapeutic molecules. One reason may be stability *in vivo* and BBB-permeability of the peptides. The present study aims to identify a novel LRP1-binding peptide for RMT, where we successfully generated a 15-mer cyclic peptide named KS-487. It explicitly bound to Cluster 4 domain of LRP1 with the binding EC_{50} value of 10.5 nM and was relatively stable in mouse plasma within 24 h. Moreover, its high BBB permeability was demonstrated using *in vitro* rat and monkey BBB models. By 24 h incubation, 13% and 17% of the added amount of KS-487 (10 μ M) penetrated rat BBB and monkey BBB, respectively. KS-487 would be a potential candidate for the LRP1-mediated transcytosis-based drug delivery to CNS, as these values were significantly higher than those of the known LRP1-binding peptides—Angiopep-2 and L57.

1. Introduction

The worldwide estimate of people with long-term central nervous system (CNS) disorders, such as schizophrenia and autism spectrum disorder, is one billion. The total economic burden in the U.S. and Europe by 2030 is estimated to be \$6 trillion [1]. Thus, developing effective treatment for CNS diseases holds an enormous market value; however, this area records the highest failure rate in the field of drug discovery [1,2]. One of the factors is the existence of the blood–brain barrier (BBB) that physically separates peripheral tissues and the brain [3]. BBB is formed around brain vessels overlapped by endothelial cells, pericytes, and astrocytes, resulting in strict regulation of the inflow/outflow of molecules between peripheral tissues and the brain. For example, it is known that molecules that passively cross the BBB from peripheral tissues prefer smaller molecular weights and higher lipophilicity [4].

Although most drug discoveries for CNS diseases have been made with low-molecular-weight compounds, there are some concerns that

small molecules could have undesirable off-target effects due to limited drug target-selectivity and that modulating protein–protein interactions is difficult with conventional small molecules [5]. In contrast, medium-size molecules (such as a peptide) and macromolecules (such as an antibody) are superior to have drug target-selectivity and to modulate protein–protein interactions compared to small molecules [6–8], but the presence of BBB makes it extremely difficult for these molecules to enter the brain passively through peripheral administrations. Thus, the establishment of a technology to transport medium-size molecules and macromolecules to CNS is eagerly awaited.

One strategy to deliver medium-size molecules and macromolecules from peripheral tissues to the brain is via receptor-mediated transcytosis (RMT) [9,10]. Transporters for glucose and amino acid substrate and receptors for insulin, transferrin, and lipoprotein have been investigated. Because transferrin receptor (TfR)-binding antibody conjugated with therapeutic molecule was launched in 2021 [11], among them, proof of concept for RMT by TfR has already been demonstrated.

Low-density lipoprotein receptor-related protein 1 (LRP1) is another

Abbreviations: BBB, blood–brain barrier; CNS, central nervous system; LRP1, low-density lipoprotein receptor-related protein 1; RMT, receptor-mediated transcytosis.

E-mail addresses: sakamoto-kotaro@ichimaru.co.jp, weidlichk58@gmail.com.

<https://doi.org/10.1016/j.bbrep.2022.101367>

Received 28 August 2022; Received in revised form 21 September 2022; Accepted 6 October 2022

2405-5808/© 2022 The Author. Published by Elsevier B.V. This is an open access article under the CC BY-NC-ND license (<http://creativecommons.org/licenses/by-nc-nd/4.0/>).

receptor for RMT [12]. It was reported that the expression levels of LRP1 at BBB correlate well among species (e.g., humans, monkeys, mice, etc.) [13]. In addition, the amino acid sequences of the ligand-binding domain: cluster 2 (CL2) and cluster 4 (CL4) of LRP1 that interact with diverse endogenous ligands are highly conserved among species [14]. Furthermore, demonstrating the safety of RMT via LRP1 in humans, a phase II human clinical trial of Angiopep-2 (ANG2; a LRP1-binding peptide)(TFFYGGSRGKRNNFKTEEY-OH)-paclitaxel conjugated molecule was completed [15–17]. In addition to ANG2, a linear 20-mer peptide L57 (TWPKHFDKHTFYLSILKLGKH-OH) binding to LRP1 was reported by Sakamoto et al. [18]. However, there are no drugs available in the market that contain a combination of ANG2 or L57 with therapeutic molecules.

It is imperative to generate new chemotypes that bind to LRP1. Through internal research, we had discovered a hit peptide. In this study, we synthesized a total of 42 peptides to conduct a structure-activity-relationship (SAR) study of the hit peptide. Among them, KS-487 was identified as the best peptide, and it showed (1) high-selectivity and high-affinity binding to human LRP1(CL4), (2) relative stability in mouse plasma within 24 h, and (3) high BBB permeability in the *in vitro* rat and monkey BBB models.

2. Materials and methods

2.1. Peptide synthesis

All peptides were synthesized at SCRUM Inc. (Tokyo, Japan) using Fmoc-based solid-phase peptide synthesis. In 5-Carboxyfluorescein (5-FAM)-labeling, Fmoc-Lys(5-FAM)-OH (5043, AAR Bioquest, CA, USA) was used, and in Biotin-labeling, Fmoc-Lys(Biot-Acp)-OH (L00835, Watanabe Chemical Industries, Hiroshima, Japan) was used. All analytical data of peptides in this report are presented in [Supplementary Table S1](#).

Synthesis of cyclized peptides by S-S, S-CH₂-S, or S-(CH₂)₃-S bond was performed according to the method described in Reference 19. The following briefly describes the synthesis method of 5FAM-KS-487 (5FAM-Pep2). After synthesis and purification of the side chain-protected linear peptide-linked resin, it was dissolved in dichloromethane and then mixed with 2% hydrazine solution for 10 min to deprotect Dde for the side chain of Lys and Odmab for the side chain of Glu. After washing, the resin was treated with trifluoroacetic acid (TFA) to deprotect the thiol group and excise the linear peptide from the resin. The peptide was purified by RP-HPLC using a SunFire C18 column (Waters Co, Milford, MA, USA). The fraction containing the product was collected and lyophilized to produce a side chain-deprotected peptide KS-487(linear), Ac-K(εNH-5FAM)-GTPCTYKY-Nle-LAE-Nle-C-OH, as a white powder with a mass spectrum of [M – H][–] 2103.906 (Calc 2103.3), purity of 73.49% and elution time on RP-HPLC (flow rate 1 mL/min) of 8.855 min under linear density gradient elution condition (a) (A/B = 80/20–10/90 for 20 min using 0.1% TFA in water as eluent A and 0.1% TFA in acetonitrile as eluent B). KS-487(linear) was dissolved in 0.1 M NH₄HCO₃ (pH 8.0) and reacted for 24–36 h at room temperature to form a disulfide bond between Cys⁵/Cys¹⁵. The peptide was purified by RP-HPLC using the SunFire C18 column. The fraction with the product was collected and lyophilized to obtain cyclic peptide KS-487, Ac-K(εNH-5FAM)-GTP-(CTYKY-Nle-LAE-Nle-C)-OH (disulfide bond cyclization with side chains of Cys⁵/Cys¹⁵), as a white powder with a mass spectrum of [M – H]⁺ 2101.886 (Calc 2101.5), purity of 100.00% and elution time on RP-HPLC (flow rate 1 mL/min) of 8.14 min under linear density gradient elution condition (a). Biotin-KS-487 and Biotin-KS-487(linear) were synthesized using a similar method. The mass spectrum was [M – H]⁺ 1969.863 (Calc 1969.3) and [M – H]⁺ 1971.794 (Calc 1971.3) with a purity of 95.18% and 95.31%, respectively. The elution time on RP-HPLC (flow rate 1 mL/min) of 6.725 min and 7.647 min, respectively, under linear density gradient elution condition (a). 5FAM-L57: Ac-K(εNH-5FAM)-GTWPKHFDKHTFYLSILKLGKH-

OH and 5FAM-ANG2: K(εNH-5FAM)-GTTFFYGGSRGKRNNFKTEEY-OH were synthesized by similar method. The mass spectrum was [M – H][–] 2846.358 (Calc 2845.0) and [M – H]⁺ 3070.886 (Calc 3069.7) with a purity of 98.89% and 95.86%, respectively.

2.2. Cell-free ELISA

Human LRP1(CL2)-Fc (2368-L2), human LRP1(CL3)-Fc (48248-L3), and human LRP1(CL4)-Fc (5395-L4) were purchased from R&D Systems (Minneapolis, MN, USA). The wells of a Nunc Maxisorp microplate (439454) were coated with goat anti-human IgG, Fcγ fragment specific polyclonal antibody (109-005-008, Jackson ImmunoResearch, PA, USA) (10 μg/mL) at 4 °C for overnight and then blocked with 0.5% BSA in PBS at 25 °C for 2 h. Fc-fused proteins (1 μg/mL) were captured using the antibody, and a biotinylated peptide solution was added to the wells. After 30 min incubation, wells were washed with PBS containing 0.1% Tween20 (PBST), and bound biotinylated peptides were detected calorimetrically using horseradish peroxidase (HRP)-conjugated streptavidin (ab7403, abcam, Cambridge, UK) and chromogenic reagent tetramethylbenzidine (34028, Thermo Fisher Scientific, MA, USA). The amount of HRP in each well was measured by absorbance at 450 nm. Binding EC₅₀ values were estimated using the equation: EC₅₀ = 10⁰[Log(A/B) × (50 – D)/(C – D) + Log(B)], where A is concentration at > 50% binding, B is the concentration at < 50% binding, C is the binding rate at concentration A, and D is the binding rate at concentration B.

For competition binding assays, nonbiotinylated peptides (dissolved in 2 mM DMSO, 1 μL) were mixed with mouse plasma (20 μL) prepared in-house. Immediately or after 24 h incubation at 37 °C, the mixture was diluted 200-fold with 0.5% BSA in PBS and added to the wells with biotinylated peptide (500 nM) in PBS containing 0.5% BSA. The final concentration of non-biotinylated peptide was 2000 nM. After 30 min incubation at 25 °C, the wells were washed with PBST, and bound biotin-peptide was detected as described above. Percent inhibition was calculated using the absorbance values from wells without LRP1(CL4)-Fc protein capturing as 100% inhibition and values from wells without 5FAM-peptide as 0% inhibition.

2.3. BBB permeability evaluation via *in vitro* BBB models

In vitro rat BBB model kit (RBT-24H) and monkey BBB model kit (MBT-24H) were purchased from PharmaCo-Cell Company (Nagasaki, Japan). Cells were incubated according to the manufacturer's manual and used to assay that TEER values were more than 150 (Ω × cm²) after confirmation. 5FAM-labeled peptides were dissolved in DMSO, diluted with the culture medium provided in the BBB kit, and added to vascular side wells. After incubation for indicated time at 37 °C and measuring TEER values, the medium in brain side wells was recovered, and the fluorescence count (Ex 493 nm/Em 517 nm) was detected using SpectraMax i3x (MOLECULAR DEVICES, CA, USA). The concentration of 5FAM-labeled peptides in the medium was determined using calibration curves. The “% input” value was calculated using the equation: % input = mole in brain side well (1000 μL)/input mole in vascular side well (200 μL).

Small interference RNA (siRNA) against rat LRP1 (4390771) [19] was purchased from Thermo Fisher Scientific. The siRNA was added to vascular side wells of rat BBB model with Lipofectamine RNAiMAX (13778030, Thermo Fisher Scientific) according to the manufacturer's instructions. After incubation for 24 h, culture medium was replaced to fresh medium including 5FAM-labeled peptide. BBB permeability of peptide was evaluated as described above.

2.4. Data analysis

JMP8 (SAS Institute Inc.) was used for the statistical analysis, and the level of significance was set at 5% (*p* < 0.05).

3. Results

3.1. Construction of competitive binding assay systems to evaluate LRP1-binding activity and stability of peptides in mouse plasma

In our internal research had attempted to design a LRP1-binding peptide from the sequences of natural ligands that reportedly bind to LRP1, such as Aprotinin [15], Bikunin [15], APP [15], and Kunitz-inhibitor precursor [15] (Fig. 1A). The method was similar to design ANG2 [15], but particularly (1) focusing on two Cys residues to linkage a consensus sequence between two Cys residues, (2) truncating amino acid residues to reduce the molecular weight, and (3) mainly substituting amino acid residues except for key residues such as C, R/G/K, F/Y, A/E, and E/K of natural ligands (Fig. 1A). As a result, XXCXXKXXLXEXC had been designed as the concept sequence, and then hit sequence TPCTYKYMLAEMC (Biotin-Pep0) had been obtained (Supplementary Table S1). Biotin-Pep0 had shown moderate binding activity to LRP1(CL4) (Supplementary Fig. S1) and moderate stability in mouse plasma (Supplementary Table S2). Its derivative Pep2—with an amino acid substitution of Methionine (Met) with Norleucine (Nle)—was used as the starting point of the SAR study (Fig. 1A). Pep2 had presented slightly superior stability than Pep0 in mouse plasma (Supplementary Table S2). Thus, a competition binding assay system was constructed to evaluate the LRP1(CL4)-binding activity and stability of peptides in mouse plasma simultaneously (Fig. 1B). In this assay, the LRP1(CL4)-binding activity of non-biotinylated peptides could be estimated as a competitive inhibition activity against the binding of the biotinylated peptide to LRP1(CL4). Both LRP1(CL4)-binding activity and stability in mouse plasma can be evaluated simultaneously (Fig. 1B), where, if the stability of the peptide is not good, non-biotinylated peptides incubated with mouse plasma for 24 h should show attenuated competitive inhibition activity. Biotinylated Pep2 (Biotin-Pep2): Ac-Lys (εNH-biotin)-Gly-TPCTYKY-Nle-LAE-Nle-C-OH (S-S bond formation

between Cys5 and Cys15) was synthesized. Lys1 for labeling and Gly2 for spacer was added to the N-terminus. Non-biotinylated peptide 5FAM-Pep2: Ac-Lys(εNH-5FAM)-Gly-TPCTYKY-Nle-LAE-Nle-C-OH (S-S bond formation between Cys5 and Cys15) was also synthesized. The assay system was designed to minimize the final concentration of plasma added to the wells. As shown in Fig. 1C, the plasma that entered the assay system had little effect on the LRP1(CL4)-binding of Biotin-Pep2 (500 nM). At 0 h incubation, the LRP1(CL4)-binding of Biotin-Pep2 (500 nM) was decreased in the 5FAM-Pep2 in a concentration-dependent manner. Binding activity of Biotin-Pep2 (500 nM) was 19.9% and 52.4% in the presence of 2000 nM and 500 nM 5FAM-Pep2, respectively, indicating that Biotin-Pep2 and 5FAM-Pep2 compete (1:1) for the LRP1(CL4)-binding (Fig. 1C). On the other hand, the LRP1(CL4)-binding of Biotin-Pep2 (500 nM) was inhibited to 50% in the presence of 5FAM-Pep2 (2000 nM) after 24 h incubation, suggesting that approximately 75% of 5FAM-Pep2 was degraded with mouse plasma (Fig. 1C).

3.2. Pep2 binds to LRP1(CL4) in both cyclic and linear forms

The SAR study of Pep2 was conducted using the competition binding assay system. Since Pep2 has a cyclic structure with an S-S bond between side chains of two Cys residues, the necessity of the peptide cyclization was first examined. At 0 h incubation, the inhibition (%) of 5FAM-Pep2 (2000 nM) was 79.4% (i.e., binding of Biotin-Pep2 was 20.6%), whereas that of 5FAM-Pep1 (a linear form of 5FAM-Pep2) (2000 nM) was 70.7%, indicating that the LRP1(CL4)-binding activity was retained even in the linear form, where the S-S bond was not formed (Fig. 2). When the S-S bond was changed to the S-CH₂-S bond or S-(CH₂)₃-S bond, the competitive inhibitory activity was 34.9% and 27.9%, respectively, relatively weaker than the linear peptide. Next, we examined D-Cys, which may improve peptide stability in plasma. Unexpectedly, the N-terminal D-Cys maintained LRP1-binding activity but not peptide

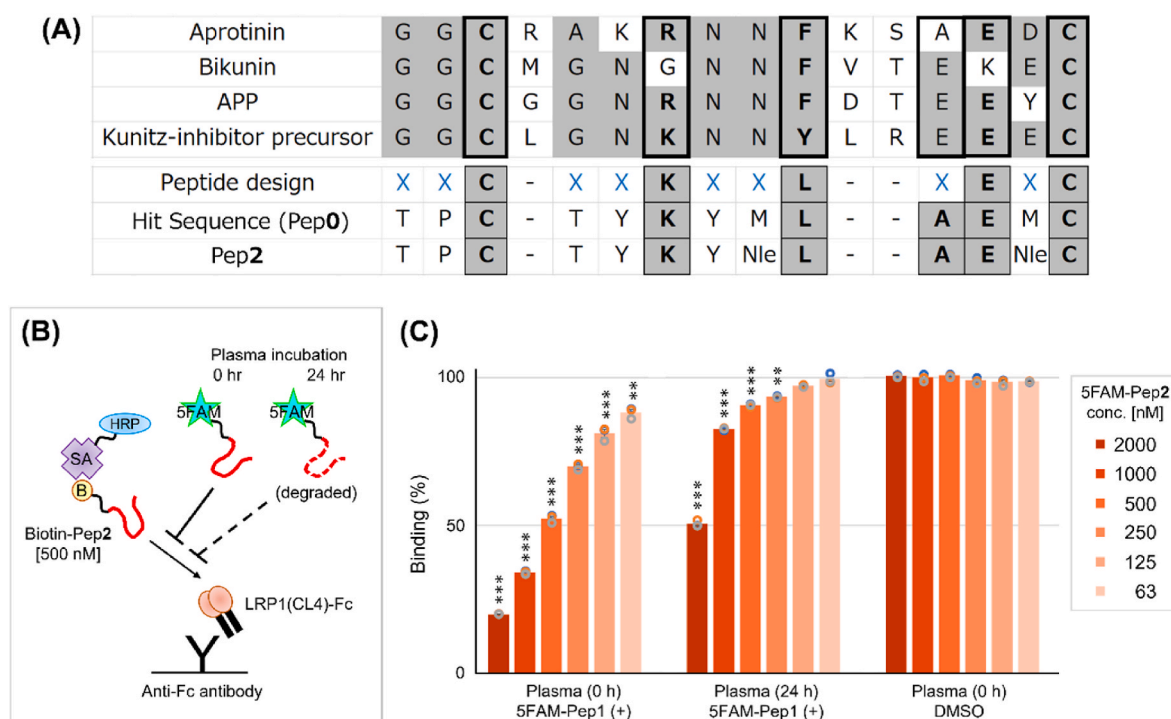


Fig. 1. Competitive binding assay for evaluation of LRP1-binding activity and stability in mouse plasma.

(A) Molecular design concept of LRP1-binding peptide (X means any amino acids). Aprotinin, Bikunin, APP, and Kunitz-inhibitor precursor are natural ligands of LRP1. The focused amino acid residues in the molecular design are shown in gray, and the key amino acid residues are indicated by bold-framed squares. (B) Schematic illustration of the competitive binding assay. (C) LRP1(CL4)-binding competition of 5FAM-Pep2 (2000–63 nM) against Biotin-Pep2 (500 nM) (n = 3, ± S.E.M, **p < 0.01, ***p < 0.001 vs. DMSO by Dunnett's test). Individual value points are indicated as circles.

Name	Cyclization	N-term														C-term	Inhibition (%)				
			1	2	3	4	5	6	7	8	9	10	11	12	13		14	15	0 h	24 h	
Pep1	None (linear)	Ac-	Lys (εNH-5FAM)	Gly	Thr	Pro	Cys	Thr	Tyr	Lys	Tyr	Nle	Leu	Ala	Glu	Nle	Cys	-OH	70.7	33.4	
Pep2	-S-S-	Ac-	Lys (εNH-5FAM)	Gly	Thr	Pro	Cys	Thr	Tyr	Lys	Tyr	Nle	Leu	Ala	Glu	Nle	Cys	-OH	79.4	48.1	
Pep3	-S-CH ₂ -S-	Ac-	Lys (εNH-5FAM)	Gly	Thr	Pro	Cys	Thr	Tyr	Lys	Tyr	Nle	Leu	Ala	Glu	Nle	Cys	-OH	34.9	2.9	
Pep4	-S-(CH ₂) ₃ -S-	Ac-	Lys (εNH-5FAM)	Gly	Thr	Pro	Cys	Thr	Tyr	Lys	Tyr	Nle	Leu	Ala	Glu	Nle	Cys	-OH	27.9	3.5	
Pep5	None (linear)	Ac-	Lys (εNH-5FAM)	Gly	Thr	Pro	D-Cys	Thr	Tyr	Lys	Tyr	Nle	Leu	Ala	Glu	Nle	Cys	-OH	13.2	6.7	
Pep6	-S-S-	Ac-	Lys (εNH-5FAM)	Gly	Thr	Pro	D-Cys	Thr	Tyr	Lys	Tyr	Nle	Leu	Ala	Glu	Nle	Cys	-OH	91.9	8.9	
Pep7	-S-CH ₂ -S-	Ac-	Lys (εNH-5FAM)	Gly	Thr	Pro	D-Cys	Thr	Tyr	Lys	Tyr	Nle	Leu	Ala	Glu	Nle	Cys	-OH	87.6	12.6	
Pep8	-S-(CH ₂) ₃ -S-	Ac-	Lys (εNH-5FAM)	Gly	Thr	Pro	D-Cys	Thr	Tyr	Lys	Tyr	Nle	Leu	Ala	Glu	Nle	Cys	-OH	54.5	15.3	
Pep9	None (linear)	Ac-	Lys (εNH-5FAM)	Gly	Thr	Pro	Cys	Thr	Tyr	Lys	Tyr	Nle	Leu	Ala	Glu	Nle	D-Cys	-OH	85.8	0.7	
Pep10	-S-S-	Ac-	Lys (εNH-5FAM)	Gly	Thr	Pro	Cys	Thr	Tyr	Lys	Tyr	Nle	Leu	Ala	Glu	Nle	D-Cys	-OH	10.6	1.4	
Pep11	-S-CH ₂ -S-	Ac-	Lys (εNH-5FAM)	Gly	Thr	Pro	Cys	Thr	Tyr	Lys	Tyr	Nle	Leu	Ala	Glu	Nle	D-Cys	-OH	14.3	0.5	
Pep12	-S-(CH ₂) ₃ -S-	Ac-	Lys (εNH-5FAM)	Gly	Thr	Pro	Cys	Thr	Tyr	Lys	Tyr	Nle	Leu	Ala	Glu	Nle	D-Cys	-OH	30.7	2.2	
Pep13	None (linear)	Ac-	Lys (εNH-5FAM)	Gly	Thr	Pro	D-Cys	Thr	Tyr	Lys	Tyr	Nle	Leu	Ala	Glu	Nle	D-Cys	-OH	42.0	9.0	
Pep14	-S-S-	Ac-	Lys (εNH-5FAM)	Gly	Thr	Pro	D-Cys	Thr	Tyr	Lys	Tyr	Nle	Leu	Ala	Glu	Nle	D-Cys	-OH	14.9	6.6	
Pep15	-S-CH ₂ -S-	Ac-	Lys (εNH-5FAM)	Gly	Thr	Pro	D-Cys	Thr	Tyr	Lys	Tyr	Nle	Leu	Ala	Glu	Nle	D-Cys	-OH	63.6	13.1	
Pep16	-S-(CH ₂) ₃ -S-	Ac-	Lys (εNH-5FAM)	Gly	Thr	Pro	D-Cys	Thr	Tyr	Lys	Tyr	Nle	Leu	Ala	Glu	Nle	D-Cys	-OH	38.6	12.7	
Pep17	-S-S-	Ac-	Lys (εNH-5FAM)	Gly	Thr	Pro	Cys	Ser	Tyr	Lys	Tyr	Nle	Leu	Ala	Glu	Nle	Cys	-OH	57.9	3.1	
Pep18		Ac-	Lys (εNH-5FAM)	Gly	Thr	Pro	Cys	cHyp	Tyr	Lys	Tyr	Nle	Leu	Ala	Glu	Nle	Cys	-OH	71.1	16.8	
Pep19		Ac-	Lys (εNH-5FAM)	Gly	Thr	Pro	Cys	tHyp	Tyr	Lys	Tyr	Nle	Leu	Ala	Glu	Nle	Cys	-OH	79.1	13.4	
Pep20		Ac-	Lys (εNH-5FAM)	Gly	Thr	Pro	Cys	Thr	Phe	Lys	Tyr	Nle	Leu	Ala	Glu	Nle	Cys	-OH	66.7	2.7	
Pep21		Ac-	Lys (εNH-5FAM)	Gly	Thr	Pro	Cys	Thr	Trp	Lys	Tyr	Nle	Leu	Ala	Glu	Nle	Cys	-OH	24.1	1.6	
Pep22		Ac-	Lys (εNH-5FAM)	Gly	Thr	Pro	Cys	Thr	His	Lys	Tyr	Nle	Leu	Ala	Glu	Nle	Cys	-OH	57.1	19.1	
Pep23		Ac-	Lys (εNH-5FAM)	Gly	Thr	Pro	Cys	Thr	Tyr	Orn	Tyr	Nle	Leu	Ala	Glu	Nle	Cys	-OH	43.4	12.6	
Pep24		Ac-	Lys (εNH-5FAM)	Gly	Thr	Pro	Cys	Thr	Tyr	Arg	Tyr	Nle	Leu	Ala	Glu	Nle	Cys	-OH	77.4	29.3	
Pep25		Ac-	Lys (εNH-5FAM)	Gly	Thr	Pro	Cys	Thr	Tyr	Lys	Nle	Nle	Leu	Ala	Glu	Nle	Cys	-OH	37.2	9.8	
Pep26		Ac-	Lys (εNH-5FAM)	Gly	Thr	Pro	Cys	Thr	Tyr	Arg	Arg	Nle	Leu	Ala	Glu	Nle	Cys	-OH	66.5	17.0	
Pep27		Ac-	Lys (εNH-5FAM)	Gly	Thr	Pro	Cys	Thr	Tyr	Lys	Tyr	Arg	Arg	Leu	Ala	Glu	Nle	Cys	-OH	37.5	4.4
Pep28		Ac-	Lys (εNH-5FAM)	Gly	Thr	Pro	Cys	Thr	Tyr	Lys	Tyr	Nle	Val	Ala	Glu	Nle	Cys	-OH	20.8	0.7	
Pep29		Ac-	Lys (εNH-5FAM)	Gly	Thr	Pro	Cys	Thr	Tyr	Lys	Tyr	Nle	Ile	Ala	Glu	Nle	Cys	-OH	12.1	0.8	
Pep30		Ac-	Lys (εNH-5FAM)	Gly	Thr	Pro	Cys	Thr	Tyr	Lys	Tyr	Nle	Nle	Ala	Glu	Nle	Cys	-OH	13.3	2.7	
Pep31		Ac-	Lys (εNH-5FAM)	Gly	Thr	Pro	Cys	Thr	Tyr	Lys	Tyr	Nle	Ahep	Ala	Glu	Nle	Cys	-OH	56.4	14.6	
Pep32		Ac-	Lys (εNH-5FAM)	Gly	Thr	Pro	Cys	Thr	Tyr	Lys	Tyr	Nle	Aoc	Ala	Glu	Nle	Cys	-OH	56.6	10.8	
Pep33		Ac-	Lys (εNH-5FAM)	Gly	Thr	Pro	Cys	Thr	Tyr	Lys	Tyr	Nle	Leu	D-Ala	Glu	Nle	Cys	-OH	67.4	17.2	
Pep34		Ac-	Lys (εNH-5FAM)	Gly	Thr	Pro	Cys	Thr	Tyr	Lys	Tyr	Nle	Leu	Aib	Glu	Nle	Cys	-OH	82.0	25.4	
Pep35		Ac-	Lys (εNH-5FAM)	Gly	Thr	Pro	Cys	Thr	Tyr	Lys	Tyr	Nle	Leu	Ala	Asp	Nle	Cys	-OH	19.6	10.1	
Pep36		Ac-	Lys (εNH-5FAM)	Gly	Thr	Pro	Cys	Thr	Tyr	Lys	Tyr	Nle	Leu	Ala	Ala	Nle	Cys	-OH	13.2	10.7	
Pep37		Ac-	Lys (εNH-5FAM)	Gly	Thr	Pro	Cys	Thr	Tyr	Lys	Tyr	Nle	Leu	Ala	Gly	Nle	Cys	-OH	9.8	9.8	
Pep38		Ac-	Lys (εNH-5FAM)	Gly	Thr	Pro	Cys	Thr	Tyr	Lys	Tyr	Nle	Leu	Ala	Glu	Val	Cys	-OH	59.4	11.0	
Pep39		Ac-	Lys (εNH-5FAM)	Gly	Thr	Pro	Cys	Thr	Tyr	Lys	Tyr	Nle	Leu	Ala	Glu	Leu	Cys	-OH	20.7	6.8	
Pep40		Ac-	Lys (εNH-5FAM)	Gly	Thr	Pro	Cys	Thr	Tyr	Lys	Tyr	Nle	Leu	Ala	Glu	Ile	Cys	-OH	24.9	10.2	
Pep41		Ac-	Lys (εNH-5FAM)	Gly	Thr	Pro	Cys	Thr	Tyr	Lys	Tyr	Nle	Leu	Ala	Glu	Ahep	Cys	-OH	11.6	11.0	
Pep42		Ac-	Lys (εNH-5FAM)	Gly	Thr	Pro	Cys	Thr	Tyr	Lys	Tyr	Nle	Leu	Ala	Glu	Aoc	Cys	-OH	16.2	12.2	

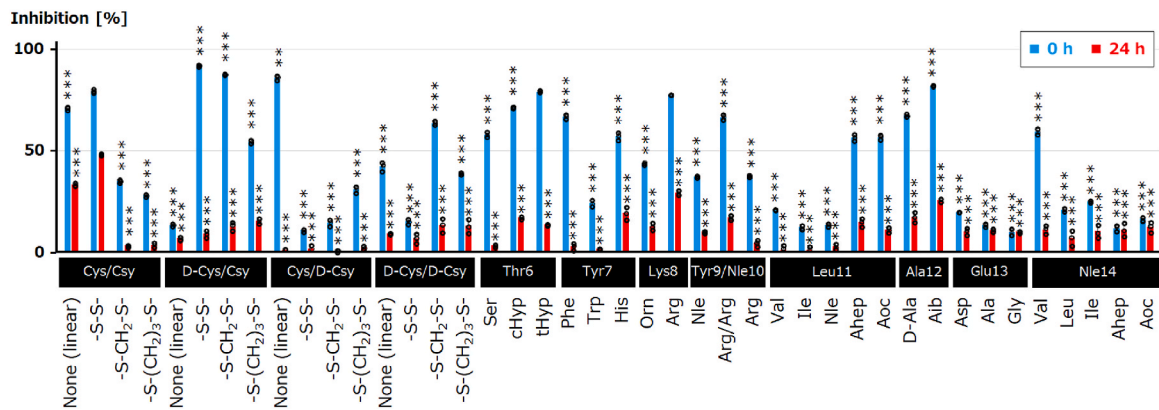


Fig. 2. Amino acid sequence and SAR study of peptides.

Peptide sequence and competitive inhibition activity against LRP1-binding of Biotin-Pep2 are shown. Inhibition (%) of 5FAM-peptide (2000 nM) with/without plasma incubation (0 h/24 h) against Biotin-Pep2 (500 nM) was calculated using the absorbance values from wells without LRP1(CL4)-Fc protein capturing as 100% inhibition and values from wells without 5FAM-peptide as 0% inhibition (n = 3, ± S.E.M, **p < 0.01, ***p < 0.001 vs. 5FAM-Pep2 by Dunnett's test). Individual value points are indicated as circles. Abbreviations; Nle, L-Norleucine; cHyp, 4-cis-Hydroxy-L-Proline; tHyp, 4-trans-Hydroxy-L-Proline; Orn, L-Ornithine; Ahep, (S)-2-Aminoheptanoic acid; Aoc, (S)-2-Amino-octanoic acid; and Aib, (S)-2-Aminoisobutylic acid.

stability, and the C-terminal D-Cys dramatically reduced LRP1-binding activity. Substitution of the N- and C-terminal Cys residues with D-Cys did not improve the binding activity or peptide stability.

3.3. Most amino acid substitutions within the cyclic structure of Pep2 either reduce LRP1(CL4)-binding activity or peptide stability except for that of Lys8Arg and Ala12Aib substitutions

The effects of substituting amino acid residues within the cyclic structure on LRP1(CL4)-binding and peptide stability in plasma were

evaluated (Fig. 2). Substitution of Thr6 to Ser, tHyp, or cHyp retained the binding activity but attenuated peptide stability. Similarly, substituting Tyr7 to Phe, Trp, or His also attenuated peptide stability. Substituting Lys8 to Arg retained both the binding activity and peptide stability. Amino acid substitutions for Tyr9 to Nle and Nle10 to Arg decreased the binding activity. Substitutions of Leu11 and Nle14 with various aliphatic amino acids uniformly reduced the binding activity. Substitution of Ala12 to Aib improved the binding activity and slightly decreased peptide stability. Substitutions of Glu13 did not improve the binding activity. Taken together, the SAR study revealed that almost all

the amino acid substitutions within the cyclic structure of Pep2 reduced LRP1(CL4)-binding activity or peptide stability.

3.4. Biotin-KS-487 and Biotin-KS-487(linear) show high affinity and selective binding to LRP1(CL4)

Since the SAR study did not find a significant sequence superior to Pep2, we assigned a code KS-487 to the Pep2 sequence: Ac-Lys(eNH-Z)-Gly-Thr-Pro-(Cys-Thr-Tyr-Lys-Tyr-Nle-Leu-Ala-Glu-Nle-Cys)-OH (S-S bond formation between Cys5 and Cys15, Z = labeling such as Biotin and 5-FAM), the best sequence identified in this study. As shown in Fig. 3, both cyclic and linear forms of biotinylated peptides demonstrated highly potent and specific binding to LRP1(CL4) in a concentration-dependent manner. They showed no binding or slight binding to other clusters such as LRP1(CL2) and LRP1(CL3). The LRP (CL4)-binding EC₅₀ values of Biotin-KS-487 and Biotin-KS-487(linear) were calculated to be 10.5 nM and 11.0 nM, respectively.

3.5. KS-487 shows superior *in vitro* BBB permeability than those of known LRP1-binding peptides ANG2 and L57

The BBB permeability of peptides was evaluated using *in vitro* BBB model (Fig. 4A)—a widely used evaluation system to predict *in vivo* BBB permeability of drug molecules—which mimics *in vivo* BBB properties (such as the expression of various receptors/transporters and the ability form tight junctions) [20]. 5-FAM-labeled peptide was added to the vascular side wells, and the medium in the brain side wells was collected after the indicated incubation time to determine the concentration of 5-FAM-labeled peptide in the medium. The concentration was determined from the fluorescence count (Ex 493 nm/Em 517 nm) and calibration curves. The “% input” value means the enrichment of 5-FAM-labeled peptide in the brain side wells and was calculated as follows: % input = mole in brain side well/input mole in vesicular side well. To begin, the BBB permeability test was examined at 30 min, a typical incubation time, however, the amount of 5-FAM-labeled peptide (1 μM input) (5FAM-KS-487 and the positive control peptides;

5FAM-L57 and 5FAM-ANG2) crossed to the brain side from the vascular side was almost the detection limit such below 0.5% (Fig. 4B). Thus, we examined 6 and 24 h incubation times. As shown in Fig. 4C, 5FAM-KS-487 (10 and 30 μM input) presented permeability across both *in vitro* rat and monkey BBBs in both peptide concentrations at all incubation time points (6 and 24 h). The % input values had tendency to shown incubation time and peptide concentration dependency. As shown in Fig. 4B, the amount of 5FAM-KS-487 that permeated the rat and monkey BBBs was relatively higher at the 24 h time point than at the 6 h time point.

Next, BBB permeability at concentrations 1, 3, and 10 μM and an incubation time of 24 h were examined. In addition, a comparison with reported BBB permeable peptides L57 and ANG2 was conducted. A total of three samples: 5FAM-KS-487, 5FAM-L57, and 5FAM-ANG2, were assessed. As shown in Fig. 4D, KS-487 demonstrated superior BBB permeability compared to ANG2 and L57 in both rat and monkey BBB models. When KS-487 was added at 10 μM, approximately 10%–15% of the added dose passed through the rat and monkey BBBs at 24 h incubation. The TEER values after 24 h incubation were more than 150 (Ω × cm²) (Supplementary Table S3), meaning barrier function was retained [20]. Namely, the BBB permeability of 5FAM-KS-487 was not due to decrease in BBB function. As shown in Supplementary Table S2, 99.6% and 28.5% of 5FAM-KS-487 was intact after 2 h and 24 h incubation in mouse plasma, respectively. On the other hand, 30.7% of 5FAM-L57 was intact after 2 h incubation in mouse plasma, but degraded to below detection limit after 24 h incubation. As shown in Supplementary Table S4, 97.1% of 5FAM-KS-487 and 89.2% of 5FAM-ANG2 were intact after 24 h incubation in culture medium of BBB kit. In addition, as presented in Fig. 4E, pre-treatment by siRNA against rat LRP1 significantly decreased BBB permeability of 5FAM-KS-487, and 5-FAM itself little permeated *in vitro* BBB. Taken together, it is likely that (1) what was detected was mainly 5-FAM that attached to KS-487 rather than 5-FAM dissociated from KS-487 and (2) 5FAM-KS-487 permeated BBB via LRP1.

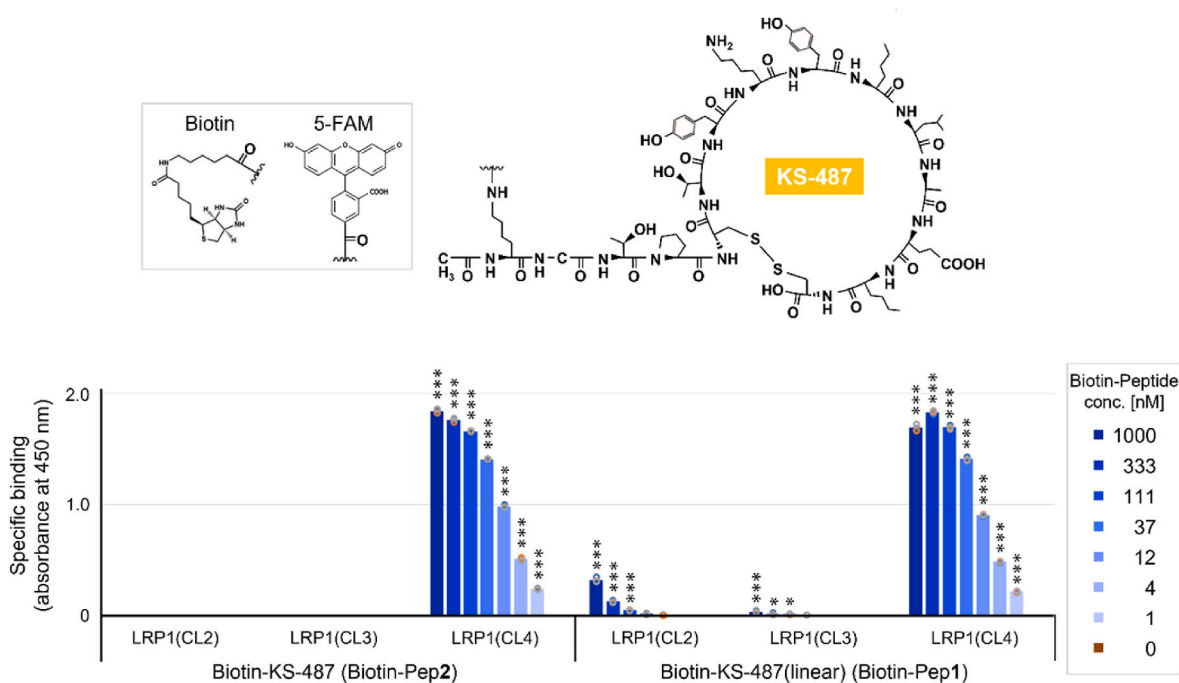


Fig. 3. Chemical structure and binding selectivity of Biotin-KS-487 and Biotin-KS-487(linear).

The results are expressed as mean ± S.E.M of n = 3 (*p < 0.05, ***p < 0.001 vs. absorbance of the well treated no Biotin-peptide by Dunnett's test). Individual value points are indicated as circles.

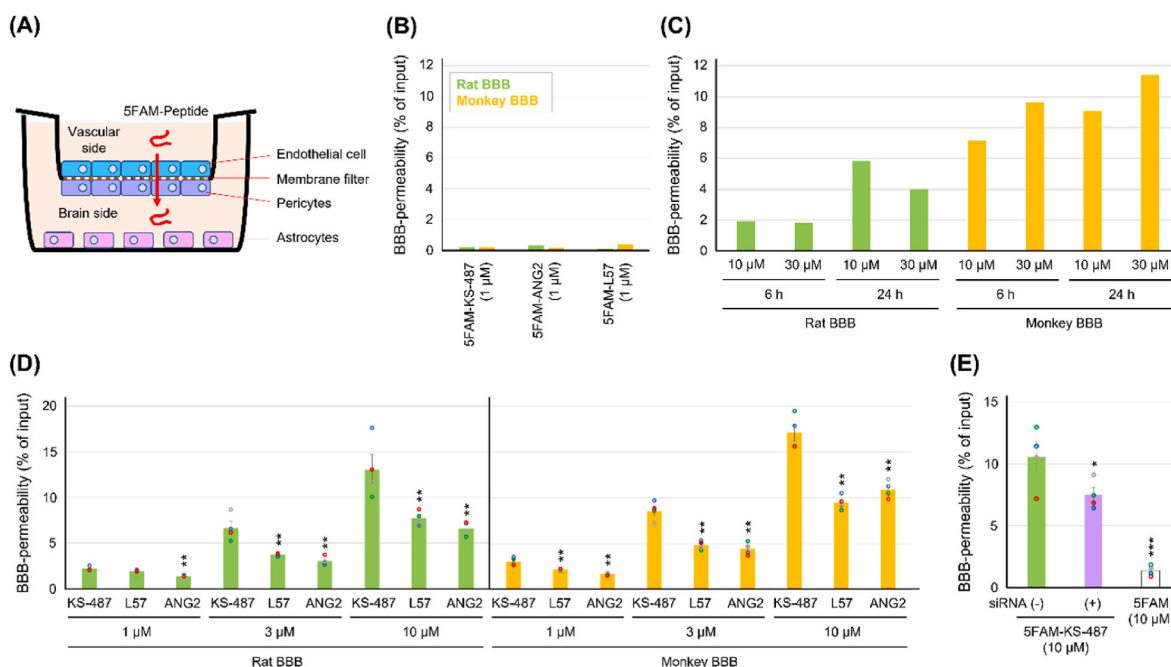


Fig. 4. BBB permeability of peptides in the *in vitro* BBB models.

(A) Schematic illustration of BBB permeability assay. (B) BBB permeability of 5FAM-labeled peptides (1 μ M) in rat BBB models for incubation time 30 min ($n = 1$). (C) BBB permeability of 5FAM-KS-487 (10 and 30 μ M) in rat and monkey BBB models for incubation time 6 h and 24 h ($n = 1$). The result was obtained by independent experiments using separately treated cultures. (D) BBB permeability of 5FAM-labeled peptides (1, 3, and 10 μ M) in rat and monkey BBB models (24 h incubation). The results are expressed as mean \pm S.E.M. of $n = 4$ independent experiments using separately treated cultures (** $p < 0.01$ vs. KS-487 by Dunnett's test). Individual value points are indicated as circles. (E) BBB permeability of 5FAM-KS-487 (10 μ M) in rat BBB model (24 h incubation) with or without pre-treatment by siRNA against rat LRP1. The results are expressed as mean \pm S.E.M. of $n = 4$ independent experiments using separately treated cultures (* $p < 0.05$, *** $p < 0.001$ vs. KS-487 by Dunnett's test).

4. Discussion

Drug discovery for CNS diseases will be greatly impacted by the effective drug delivery system (DDS) targeting brain tissue, which allows mid-size molecules and macromolecules administered from peripheral tissues to penetrate brain tissue. To establish the DDS, various types of RMT have been considered. Compatibility between the delivery and therapeutic molecules is a key component of drug discovery employing DDS. Therefore, even if the peptides bind to the same receptor but with different chemotypes, is meaningful. In this study, we successfully generated a novel cyclic peptide KS-487 for RMT via LRP1. Although linear peptides ANG2 and L57 have been reported as LRP1-binding peptides, high affinity/specificity to LRP1 ($EC_{50} = 10$ nM) and relative stability in mouse plasma (49.9% residual rate within 24 h in mouse plasma) are two benefits of KS-487. For example, L57 reportedly showed an LRP1-binding EC_{50} value of 45 nM and cross-reactivity to LRP1 (CL2) [18]. It was degraded below detection limit within 24 h in mouse plasma (Supplementary Table S2). Not only peptide stability in plasma but also *in vivo* pharmacokinetics are important to deliver sufficient drug doses to the brain via RMT. Generally, peptide administered from peripheral tissues is degraded by protease and eliminated early by kidneys; thus, their half-life ($t_{1/2}$) in the blood is from a few minutes to several tens of minutes [21]. Since sufficient BBB permeability of KS-487 *in vitro* required at least approximately 6–24 h incubation (Fig. 4), sufficient BBB permeability *in vivo* would also require at least several hours to 24 h blood retention. KS-487 is not expected to be readily degraded in the blood, whereas is expected to undergo early renal clearance. The elimination $t_{1/2}$ of KS-487 is probably less than 1 h, but depending on the combination with therapeutic molecules, the elimination $t_{1/2}$ of KS-487 may be possible to extend.

The intriguing thing is that, whereas S-CH₂-S and S-(CH₂)₃-S- were not tolerated, the peptide sequence of KS-487 retained LRP1-binding activity in both linear and cyclic forms (S-S bond). According to the

materials and methods section, the retention times in purification RP-HPLC in Biotin-KS-487 and Biotin-KS-487(linear) were different as 6.725 min and 7.645 min, indicating that the conformation of peptides would vary to some extent depending on the presence or absence of S-S bond formation. Since LRP1 (CL4) is known to bind a variety of endogenous ligands [14,15], it is likely that the structure of CL4 is flexible and allows interaction even if peptide conformation changes to some extent. On the other hand, amino acid substitutions within the peptide's cyclic structure decreased its ability to attach to LRP1 (CL4), indicating that the peptide interacts with LRP1 (CL4) in a particular way. One of the future efforts will be to clarify the binding mode between KS-487 and LRP1 (CL4).

Peptide sequences should be used in DDS for both fusion and conjugation. Although KS-487 contains unnatural amino acid residue Nle, the parental hit peptide sequence exclusively comprises natural amino acids. Thus the hit peptide sequence is easily converted into biologics by protein production if it is fused to the N-/C-terminus or grafted into the loop region of a therapeutic protein, such as an enzyme or an antibody. In near future, we will evaluate whether KS-487 can be used as a transporter *in vivo* for larger therapeutic molecules such as an antibody. Most significantly, we created KS-487, a novel LRP1-binding peptide, and showed that it significantly increases BBB permeability in BBB models using rats and monkeys. KS-487 has the potential to be an effective DDS tool for targeting brain tissue, even though more research (and conjugation with therapeutic molecules) is required to assess its physiological effects. It would aid in the future development of RMT-based drugs for treating CNS diseases.

Declaration of competing interest

This research received no external funding. The author has no conflict of interest to declare.

Data availability

Data will be made available on request.

Appendix A. Supplementary data

Supplementary data to this article can be found online at <https://doi.org/10.1016/j.bbrep.2022.101367>.

References

- [1] Larry Ereshefsky, Rebecca Evans, Rohit Sood, Doug Williamson, Brett A. English, Venturing into a new era of CNS drug development to improve success, *YOUR JOURNEY. OUR MISSION* (2015).
- [2] Valentin K. Gribkoff, Leonard K. Kaczmarek, The need for new approaches in CNS drug discovery: why drugs have failed, and what can be done to improve outcomes, *Neuropharmacology* 120 (2017) 11–19.
- [3] Hossam Kadry, Behnam Noorani, Luca Cucullo, A blood-brain barrier overview on structure, function, impairment, and biomarkers of integrity, *Fluids Barriers CNS* 17 (1) (2020) 69.
- [4] William A. Banks, Characteristics of compound that cross the blood-brain barrier, *BMC Neurol.* 9 (Suppl 1) (2009) S3.
- [5] Haiying Lu, Qiaodan Zhou, Jun He, Zhongliang Jiang, Peng Cheng, Rongsheng Tong, Jianyou Shi, Recent advances in the development of protein-protein interactions modulators: mechanisms and clinical trials, *Signal Transduct. Targeted Ther.* 5 (1) (2020) 213.
- [6] Kotaro Sakamoto, Teruaki Masutani, Takatsugu Hirokawa, Generation of KS-58 as the first K-Ras(G12D)-inhibitory peptide presenting anti-cancer activity in vivo, *Sci. Rep.* 10 (1) (2020), 21671.
- [7] Kotaro Sakamoto, Lu Chen, Tatsunori Miyaoka, Mei Yamada, Teruaki Masutani, Kenji Ishimoto, Nobumasa Hino, Shinsaku Nakagawa, Satoshi Asano, Yukio Ago, Generation of KS-133 as a novel bicyclic peptide with a potent and selective VIPR2 antagonist activity that counteracts cognitive decline in a mouse model of psychiatric disorders, *Front. Pharmacol.* 12 (2021), 751587.
- [8] Fern Sha, Salzman Gabriel, Ankit Gupta, Shohei Koide, Monobodies and other synthetic binding proteins for expanding protein science, *Protein Sci.* 26 (5) (2017) 910–924.
- [9] Jason M. Lajoie, Eric V. Shusta, Targeting receptor-mediated transport for delivery of biologics across the blood-brain barrier, *Annu. Rev. Pharmacol. Toxicol.* 55 (2015) 613–631.
- [10] Magdalena Markowicz-Piasecka, Agata Markiewicz, Patrycja Darlak, Joanna Sikora, Santosh Kumar Adla, Sreelatha Bagina, Kristiina M. Huttunen, Current chemical, biological, and physiological views in the development of successful brain-targeted pharmaceuticals, *Neurotherapeutics* (2022), <https://doi.org/10.1007/s13311-022-01228-5>.
- [11] Ryuji Yamamoto, Satoshi Kawashima, Pharmacological property, mechanism of action and clinical study results of Pabinafusp Alfa (Genetical Recombination) (IZCARGO ® I.V. Infusion 10 mg) as the therapeutic for Mucopolysaccharidosis type-II (Hunter syndrome), *Nihon Yakurigaku Zasshi* 157 (1) (2022) 62–75.
- [12] Xiaohe Tian, Sophie Nyberg, Paul S. Sharp, Jeppe Madsen, Nooshin Daneshpour, Steven P. Armes, Jason Berwick, Mimoun Azzouz, Pamela Shaw, N Joan Abbott, Giuseppe Battaglia, LRP-1-mediated intracellular antibody delivery to the Central Nervous System, *Sci. Rep.* 5 (2015), 11990.
- [13] Sumio Ohtsuki, Yasuo Uchida, Yoshiyuki Kubo, Tetsuya Terasaki, Quantitative targeted absolute proteomics-based ADME research as a new path to drug discovery and development: methodology, advantages, strategy, and prospects, *J. Pharmaceut. Sci.* 100 (9) (2011) 3547–3559.
- [14] Nicola Potere, Marco Giuseppe Del Buono, Adolfo Gabriele Mauro, Antonio Abbate, Stefano Toldo, Low density lipoprotein receptor-related protein-1 in cardiac inflammation and infarct healing, *Front. Cardiovasc. Med.* 6 (2019) 51.
- [15] Michel Demeule, Régina Anthony, Christian Ché, Poirier Julie, Tran Nguyen, Reinhard Gabathuler, Jean-Paul Castaigne, Richard Béliveau, Identification and design of peptides as a new drug delivery system for the brain, *J. Pharmacol. Exp. Therapeut.* 324 (3) (2008) 1064–1072.
- [16] Drappatz Jan, Andrew Brenner, Eric T. Wong, April Eichler, David Schiff, Morris D. Groves, Tom Mikkelsen, Steve Rosenfeld, John Sarantopoulos, Christina A. Meyers, Robert M. Fielding, Elian Kelly, Xiaolin Wang, Betty Lawrence, Mona Shing, Stephen Kelsey, Jean Paul Castaigne, Patrick Y. Wen, Phase I study of GRN1005 in recurrent malignant glioma, *Clin. Cancer Res.* 19 (6) (2013) 1567–1576.
- [17] Kumthekar Priya, Shou-Ching Tang, Andrew J. Brenner, Santosh Kesari, David E. Piccioni, Carey Anders, Jose Carrillo, Pavani Chalasani, Peter Kabos, Puhalla Shannon, Katherine Tkaczuk, Agustin A. Garcia, S Ahluwalia Manmeet, Jeffrey S. Wefel, Nehal Lakhani, Nuha Ibrahim, ANG1005, a brain-penetrating peptide-drug conjugate, shows activity in patients with breast cancer with leptomeningeal carcinomatosis and recurrent brain metastases, *Clin. Cancer Res.* 26 (12) (2020) 2789–2799.
- [18] Kotaro Sakamoto, Tokuyuki Shinohara, Yusuke Adachi, Taiji Asami, Tetsuya Ohtaki, A novel LRP1-binding peptide L57 that crosses the blood brain barrier, *Biochem. Biophys. Rep.* 12 (2017) 135–139.
- [19] Kaoru Yamada, Tadafumi Hashimoto, Chiori Yabuki, Yusuke Nagae, Masanori Tachikawa, Dudlkey K. Strickland, Qiang Liu, Guojun Bu, Lacob M. Basak, David M. Holtzman, Sumio Ohtsuki, Tetsuya Terasaki, Takeshi Iwatsubo, The low density lipoprotein receptor-related protein 1 mediates uptake of amyloid beta peptides in an in vitro model of the blood-brain barrier cells, *J. Biol. Chem.* 283 (50) (2008) 34554–34562.
- [20] Fuyuko Takata, Shinya Dohgu, Atsushi Yamauchi, Junichi Matsumoto, Takashi Machida, Kayoko Fujishita, Keisuke Shibata, Youichi Shinozaki, Kaoru Sato, Yasufumi Kataoka, Schuichi Koizumi, In vitro blood-brain barrier models using brain capillary endothelial cells isolated from neonatal and adult rats retain age-related barrier properties, *PLoS One* 8 (1) (2013), e55166.
- [21] Huizi Wu, Jiaguo Huang, Optimization of protein and peptide drugs based on the mechanisms of kidney clearance, *Protein Pept. Lett.* 25 (6) (2018) 514–521.